Title: Production and Purification of Research Scale ^{161}Tb Using Cation-Exchange Semi-Preparative HPLC for Radiopharmaceutical Applications

Short title: Purification of Reactor-Produced ^{161}Tb via Cation-Exchange HPLC

Patrick Bokolo[1], Madhushan Serasinghe[1], Marina Kuchuk[2], Jim Guthrie[2], Mary Embree[2], Stacy Wilder[2], Dmitri G. Medvedev[3], Cathy S. Cutler[3], D. Scott Wilbur[4], Yawen Li[4], Carolyn J. Anderson[1,5,6,7], Silvia S. Jurisson[1], Heather M. Hennkens[1,2*]

1. Department of Chemistry, University of Missouri, Columbia, 65211, MO, USA
2. Research Reactor Center (MURR), University of Missouri, Columbia, 65211, MO, USA
3. Isotope Research and Production Department, Brookhaven National Laboratory, Upton, 11973, NY, USA
4. Department of Radiation Oncology, University of Washington, Seattle, 98195, WA, USA
5. Department of Radiology, University of Missouri, Columbia, 65211, MO, USA
6. Molecular Imaging and Theranostics Center, University of Missouri, Columbia, 65211, MO, USA
7. Ellis Fischel Cancer Center, University of Missouri, Columbia, 65211, MO, USA

* Author to whom correspondence should be addressed.
E-Mail: HennkensH@missouri.edu; Address: Department of Chemistry, University of Missouri, 601 South College Avenue, Columbia, MO, 65211, United States

This manuscript has a 6799-word count, 5 tables, 8 figures and contains supplementary material (as a separate file).

Abstract

Terbium-161 (^{161}Tb) is emerging as a promising radionuclide for cancer therapy due to its favorable nuclear properties that are similar to clinically established lutetium-177 (^{177}Lu) along with its therapeutic edge arising from the higher number of Auger and conversion electrons per decay. These low energy electrons result in higher cytotoxicity within a short range of the decaying nuclei to enhance therapeutic efficacy. Despite these promising characteristics, a significant challenge remains in the lack of a domestic ^{161}Tb supply in the United States, which poses an obstacle to the advancement of ^{161}Tb-based radiopharmaceutical research and development. This study developed a reliable cation-exchange high-performance liquid chromatography-based method for purification of reactor-produced ^{161}Tb at quantities suitable to support research and preclinical studies. The purified ^{161}Tb product showed high radionuclidic purity with excellent radiochemical purity, and the successful labeling studies with the DOTA chelator and DOTA-TATE peptide demonstrated the effective incorporation of the purified ^{161}Tb into radiopharmaceuticals designed for targeted cancer therapy.

Keywords: alpha-hydroxyisobutyric acid; cation-exchange resin; high-performance liquid chromatography; lanthanide separation; nuclear medicine; terbium-161

1. INTRODUCTION

The recent U.S. Food and Drug Administration (FDA) approvals of two radiopharmaceuticals, NETSPOT™ ([^{68}Ga]Ga-DOTA-TATE) and LUTATHERA® ([^{177}Lu]Lu-DOTA-TATE), have established the effectiveness of using theranostic radionuclides in the diagnosis and treatment of gastroenteropancreatic neuroendocrine tumors (GEP-NETs).[1,2] Another successful application of theranostic pairing is demonstrated by the FDA approvals of prostate-specific membrane antigen (PSMA)-targeting radiopharmaceuticals for prostate cancer patients. LOCAMETZ® ([^{68}Ga]Ga-PSMA-11) was approved for use in Positron Emission Tomography (PET) imaging to detect PSMA-positive prostate lesions, including for identification of patients with metastatic prostate cancer who might potentially benefit from therapy with PLUVICTO™ ([^{177}Lu]Lu-PSMA-617).[3] These advancements have highlighted the potential for development of similar theranostic agents with other radionuclide pairings and for other types of cancer, such as breast and lung cancers.[4]

Terbium-161, which can be produced from neutron irradiation of ^{160}Gd,[5] has recently gained significant interest in the field of nuclear medicine as a potential radionuclide for cancer therapy. This interest is due to its favorable nuclear properties, which include a relatively long half-life (6.95 days), moderate beta minus particle energy (E_{β^-max} = 0.59 MeV), and low energy gamma emissions (Table 1). These properties are similar to those of clinically established ^{177}Lu (half-life = 6.64 days, E_{β^-max} = 0.50 MeV, low abundance gamma emission; Table 1). However, ~10 times the number of Auger and conversion electrons are emitted per ^{161}Tb decay (vs. ^{177}Lu), which may enable the treatment of small cancerous lesions and circulating tumor cells.[5] Moreover, terbium has two additional radioisotopes with suitable

nuclear decay properties for true theranostic pairing with ^{161}Tb: ^{152}Tb for PET imaging and ^{155}Tb for Single Photon Emission Computed Tomography (SPECT) imaging. Unlike with the current ^{68}Ga/^{177}Lu theranostic pairing, the ^{152}Tb/^{161}Tb and ^{155}Tb/^{161}Tb pairs both offer elementally matched pairings, with the latter holding the promise of generating elementally matched theranostic radiopharmaceuticals with half-lives that are also well matched (Table 1). [Place Table 1 near here]

Table 1: Properties and Nuclear Medicine Applications of ^{68}Ga, ^{177}Lu, ^{152}Tb, ^{155}Tb, and ^{161}Tb.[6]

Property	Gallium-68	Lutetium-177	Terbium-152	Terbium-155	Terbium-161
Half-life	67.7 min	6.65 d	17.5 h	5.32 d	6.95 d
Decay mode (branching ratio)	EC/β^+ (100%)	β^- (100%)	EC/β^+ (100%)	EC (100%)	β^- (100%)
Beta particle energy, $E_{\beta max}$	1.9 MeV	0.50 MeV	3.0 MeV	none	0.59 MeV
Gamma emissions[a] (abundance)	1077 keV (3%)	208 keV (10%)	344 keV (64%)	87 keV (32%) 105 keV (25%)	26 keV (23%) 49 keV (17%) 75 keV (10%)
Application	Established for PET imaging	Established for cancer therapy	Promising for PET imaging	Promising for SPECT imaging	Promising for cancer therapy

[a] Gammas with intensities ≥10% are listed. If none, the highest abundance gamma is listed.

Preclinical SPECT/Computed Tomography (CT) imaging studies of ^{155}Tb-labeled peptides (specifically the minigastrin analogue [^{155}Tb]Tb-MD and the somatostatin analogue [^{155}Tb]Tb-DOTA-TATE) in mice with tumors demonstrated significant accumulations of radioactivity within the tumor xenografts, with excellent imaging quality achieved on a small animal scanner despite the low amount of radioactivity used (0.1-0.2 mCi, 4.2-8.5 MBq).[7] These findings suggest that imaging with ^{155}Tb could be viable for dosimetry planning prior

to therapeutic interventions involving rare earth radionuclides such as ^{90}Y, ^{177}Lu, ^{166}Ho, and ^{161}Tb. While a comparison study of [^{161}Tb]Tb-PSMA-617 and [^{177}Lu]Lu-PSMA-617 showed similar *in vitro* properties in terms of binding (K_d) and cell internalization, the [^{161}Tb]Tb-PSMA-617 was up to three times more effective than [^{177}Lu]Lu-PSMA-617 in reducing the viability and survival of PSMA-positive PC-3 PIP tumor cells.[8] Further, [^{161}Tb]Tb-PSMA-617 demonstrated activity-dependent tumor growth inhibition and prolonged survival of PC-3 PIP tumor-bearing mice with no detectable side effects in the treatment.[8]

Similarly, conjugates of radiolabeled folate, [^{161}Tb]Tb-cm09 and [^{177}Lu]Lu-cm09, exhibited comparable SPECT imaging characteristics in phantom studies, while [^{161}Tb]Tb-cm09 showed an improved therapeutic efficacy in inhibiting cancer cell growth *in vitro*.[9] *In vivo* studies with tumor-bearing mice also showed favorable results for [^{161}Tb]Tb-cm09 in terms of imaging and biodistribution.[9] Further, in the first-in-human clinical SPECT imaging of a ^{161}Tb radiopharmaceutical, [^{161}Tb]Tb-DOTA-TOC, the distribution profiles for [^{161}Tb]Tb-DOTA-TOC and [^{177}Lu]Lu-DOTA-TOC were similar.[10] These and other studies[10,11] have demonstrated the clinical promise of ^{161}Tb as an alternative to, and possibly superior to, the clinically established ^{177}Lu.

However, despite the potential application of ^{161}Tb for cancer therapy, there is an insufficient supply of this radionuclide, particularly from the United States, which poses a significant obstacle to advancing research and development of ^{161}Tb-based radiopharmaceuticals for nuclear medicine applications. Isolating ^{161}Tb from both the Gd target material and co-produced radionuclidic impurities is critical since the presence of either in the ^{161}Tb product would hinder its use in nuclear medicine, both in preclinical and

clinical settings.[12] Due to the similar physical and chemical properties of the lanthanide (Ln) elements, chemical separation of Tb from Gd is challenging.[13] There have been several reports on various techniques for separating neighboring lanthanides.[14–18] Using a cation-exchange resin in conjunction with alpha-hydroxyisobutyric acid (α-HIBA) as a complexing and eluting agent has produced promising results.[18] This separation takes advantage of the stability constant differences of lanthanides with α-HIBA.[19] Lanthanides with more stable complexes are eluted first, followed by those with less stable complexes. The ionic radius strongly influences the complexation of Ln^{3+} with α-HIBA, with lanthanides of smaller ionic radii more likely to form stable complexes. Thus, Tb^{3+} with its smaller ionic radius (92.3 pm) than Gd^{3+} (93.8 pm) forms the more stable complex with α-HIBA and is eluted with α-HIBA before Gd^{3+}. Therefore, in this study, we have developed a cation-exchange based isolation method for the purification of ^{161}Tb from neutron irradiated $[^{160}Gd]Gd(NO_3)_3$ targets. We then assessed the quality of the purified ^{161}Tb as well as its suitability for labeling of the DOTA chelator and the DOTA-TATE peptide.

2. MATERIALS AND METHODS

2.1 Chemicals and Instrumentation

All acids were Optima™ grade and were purchased from Fisher Scientific (Fair Lawn, NJ) and Sigma-Aldrich (St. Louis, MO). DOTA (1,4,7,10-tetraazacyclododecane-1,4,7,10-tetraacetic acid, purity of ≥95%) and DOTA-TATE (DOTA-D-Phe-c(Cys-Tyr-D-Trp-Lys-Thr-Cys)-Thr(OH)); purity of 97.77%) were procured from Macrocyclics™ (Plano, TX) and Creative Peptides (Shirley, NY), respectively. Gadolinium oxide ($[^{160}Gd]Gd_2O_3$) target material with 98.2% isotopic enrichment was obtained from Trace Sciences International

(Wilmington, DE). Supplementary Material Table S1 contains information regarding the elemental impurities of the [^{160}Gd]Gd_2O_3 material. Ultrapure water (18.2 MΩ) from an ELGA PURELAB Pulse 1/Flex 2 system (Veolia/ELGA LabWater, Woodridge, IL) outfitted with a 0.2 μm point-of-use filter was employed throughout these studies unless otherwise specified.

Analytical and radioanalytical high-performance liquid chromatography (HPLC) analyses were conducted on a Shimadzu HPLC system outfitted with the following components: FCV-11AL Shimadzu valve unit, DGU-20A 2R degassing unit, SCL-10A VP Shimadzu system controller, and SPD-20AV Shimadzu Prominence UV/Vis Photodiode Array (PDA) detector. The HPLC was connected in-line to a NaI(Tl) detector. Live-time chromatogram visualization was performed with Shimadzu's Lab Solution software. For ^{161}Tb isolation, cation-exchange Dionex IonPac™ CS3 semi-preparative (9 mm x 250 mm; Dionex, Sunnyvale, CA) and guard columns were utilized. For further processing of the HPLC-isolated ^{161}Tb, the following Eichrom resins were used: LN (LaNthanides), composed of di(2-ethylhexyl) orthophosphoric acid (HDEHP), particle size 100-150 μm (part number LN-B50-S); PF (Pre-Filter), particle size 100-150 μm (part number PF-B01-A); and RE (Rare Earth), composed of octyl(phenyl)-*N*,*N*-di-isobutyl carbamoyl-methyl phosphine oxide (CMPO) in tributyl phosphate (TBP), particle size 100-150 μm (part number RE-B25-S).

At each stage from target characterization through final product assessment, radionuclide identity along with ^{161}Tb purity and activity measurements were made using an ORTEC High Purity Germanium (HPGe) GEM2070 detector (Oak Ridge, TN) equipped with a multichannel analyzer (Canberra Digital Signal Analyzer DSA-LX) and Canberra Genie 2000 gamma analysis software. This system has a relative efficiency of 23% and a peak-to-

Compton ratio of 57:1 with Full Width at Half Maximum (FWHM) resolution of 1.72 keV at 1.33 MeV (^{60}Co). Activity measurements made with the HPGe detector utilized the 88 keV gamma line of ^{161}Tb for quantification. The detector's energy resolution enabled clear peak discrimination, with 600-sec acquisition times ensuring reliable counting statistics. A Capintec Radioisotope Calibrator CRC-7 with a calibration setting of 209 and a factor of 1 was also utilized to monitor the activity of ^{161}Tb solutions.

Radio thin layer chromatography (radioTLC) analyses were conducted using an Eckert & Ziegler Radiopharma, Inc. (Hopkinton, MA) model B-AR-2000-2 TLC scanner, equipped with the Winscan 3.0 AR-2000 software. The efficiency of [^{161}Tb]Tb-DOTA-TATE radiolabeling was assessed on a BetaBasic™ C18 analytical HPLC column (4.6 mm x 140 mm, 3 μm) outfitted with a guard column (10 mm x 4.0 mm, 3 μm). For non-radioactive Tb-DOTA-TATE characterization, high-resolution electrospray ionization mass spectrometry (HRMS) was conducted using an LTQ Orbitrap XL mass spectrometer. The mass spectrometry data were processed with Xcalibur Qual Browser, version 2.2 (Thermo Fisher Scientific).

2.2 Target Preparation

Accurately weighed enriched [^{160}Gd]Gd_2O_3 (98.2% isotopic enrichment) was converted to [^{160}Gd]$Gd(NO_3)_3$ by dissolving into a 1 M HNO_3 solution. Following dissolution, aliquots containing the desired ^{160}Gd mass were transferred into 4 x 6 mm quartz ampoules and dried under vacuum. The ampoules containing the [^{160}Gd]$Gd(NO_3)_3$ solid were then sealed with a flame torch.

2.3 Thermal Neutron Irradiation and Dissolution of [^{160}Gd]Gd(NO_3)$_3$ Target

Enriched [^{160}Gd]Gd(NO_3)$_3$ targets, each containing ~1 mg of ^{160}Gd sealed in a quartz ampoule, were irradiated for ~7 days in a flux trap position (nominal thermal neutron flux of 1.76×10^{14} n·cm^{-2}·sec^{-1}) of the 10-MW University of Missouri Research Reactor (MURR). Following irradiation, the quartz ampoules were opened inside of a glovebox. The irradiated target material was then dissolved in 500 µL of 0.1 M HCl and transferred into an acid-washed 1.5 mL plastic microcentrifuge tube. The ^{161}Tb activity was measured in a Capintec dose calibrator. HPGe spectroscopy identified and quantified the desired ^{161}Tb product and co-produced radioactive impurities.

2.4 HPLC Isolation of ^{161}Tb from ^{160}Gd Target Material

The experimental design flow for ^{161}Tb isolation through formulation is shown in Figure 1, with additional experimental details provided below and in sections 2.5 and 2.6. About 8 hours after the end of irradiation, isolation of ^{161}Tb from ^{160}Gd and radionuclidic impurities (collected as waste) was achieved using a semi-preparative Dionex Ion Pac CS3 cation-exchange column and mobile phases of 18.2 MΩ water (mobile phase 1) and 0.6 M α-HIBA in water (mobile phase 2; pH = 3.3). To remove metal contaminants, the mobile phases were pretreated with the Chelex 100 resin (styrene-divinylbenzene copolymer paired with iminodiacetic acid group). Briefly, one liter of each mobile phase was stirred with 10 mL of Chelex resin slurry (~0.6 g in 0.1 M HNO_3), and the mixture was allowed to settle in the refrigerator (4 °C) for 2 days. Following pretreatment, the resin was removed from the 18.2 MΩ water and 0.6 M α-HIBA mobile phases via vacuum-assisted filtration through 0.22 µm membrane and nylon filters, respectively.

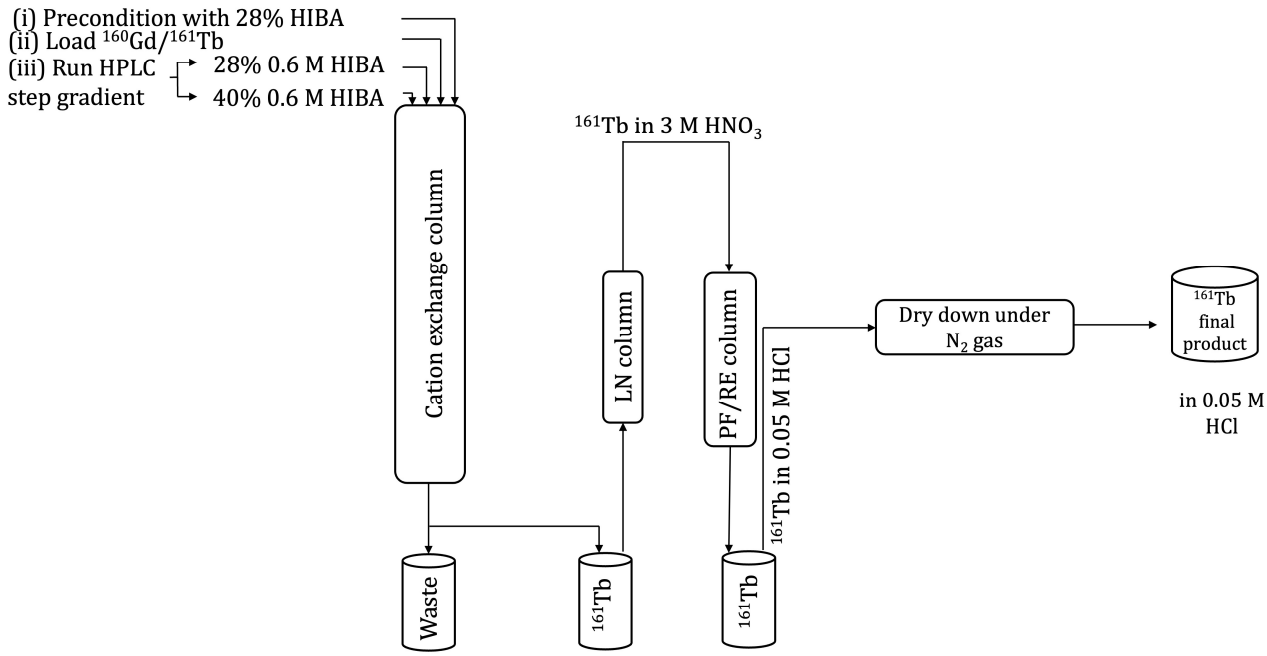

Figure 1: Experimental design flow for isolating no-carrier-added ^{161}Tb.

After loading an aliquot of the target solution onto the column, the HPLC was run at 3 mL/min in isocratic mode with mobile phase conditions of 28% mobile phase 2 in mobile phase 1. After 15 min, mobile phase 2 was increased to 40%, and the HPLC run was continued in isocratic mode under these conditions through 120 min. An aliquot of each radiolanthanide peak isolated during the run was collected and analyzed with the HPGe detector to determine the radionuclide(s) present.

2.5 Post-HPLC Column Purification with LN and RE/PF Resins

After the HPLC separation, an LN resin column was utilized to both concentrate the ^{161}Tb solution and switch the solvent from α-HIBA to HNO_3. The LN column was prepared by introducing the LN resin (0.38 g in 10 mL of 0.1 M HNO_3) into an empty plastic Bio-Rad Poly-Prep® chromatography column with a bottom frit (part number 7311550) and allowing the resin to settle under gravity flow. LN resin was added in this manner until the resin bed's

post-settling level corresponded to the 1 mL mark, after which a top frit was added to the column. The column was then rinsed several times as follows: with water until the eluant's pH exceeded 4 followed by 10 mL of 1 M ascorbic acid, then with water again until the eluant's pH was above 4 followed by 5-10 mL of 3 M HNO_3, and finally with water again until the eluant's pH was greater than 4 followed by 5 mL of 0.05 M HCl. The column was pre-equilibrated before loading by rinsing with water until the eluant's pH was greater than 4. The ^{161}Tb isolated by HPLC was then loaded onto the LN column, after which the column was washed with 3 mL water, followed by elution of ^{161}Tb in 3 M HNO_3.

A RE/PF column was utilized to further concentrate the ^{161}Tb solution, to switch the solvent from 3 M HNO_3 to 0.05 M HCl, and to remove organic impurities. First, PF resin (0.2 g in 10 mL of 0.1 M HNO_3) was introduced into an empty Bio-Rad column with a bottom frit and allowed to settle to the 0.8 mL mark. About 2 mL of water was then passed through the column to ensure an even PF resin bed. Next, RE resin (0.3 g in 10 mL of 0.1 M HNO_3) was introduced into the PF packed column and allowed to settle to the 1.6 mL mark. The top frit was gently placed on the resin bed without compressing the column. Afterward, the frit and column were rinsed several times as follows: with water until the eluant's pH exceeded 4 followed by 10 mL of 1 M ascorbic acid, then with water again until the eluant's pH was above 4 followed by 5 mL of 0.05 M HCl. The column was pre-equilibrated prior to loading by first rinsing with water until the pH was higher than 4 and then with 5 mL of 3 M HNO_3. After loading the ^{161}Tb eluant from the LN column onto the RE/PF column, the column was washed with 3 mL of 3 M HNO_3 prior to eluting the ^{161}Tb in 0.05 M HCl.

2.6 Final ^{161}Tb Solution Formulation

The ^{161}Tb fractions collected from the RE/PF column step were combined into a silanized glass vial (see Supplementary Material for the silanization procedure). The ^{161}Tb solution was evaporated to dryness under N_2 gas with gentle heating and then immediately reconstituted in 400 µL of 0.05 M HCl. The dry down and reconstitution steps were repeated twice, with a final reconstitution volume of 150 µL of 0.05 M HCl.

2.7 Determination of Radiochemical Purity and Radionuclidic Purity of the Final [^{161}Tb]$TbCl_3$ Product

The radiochemical purity of the final [^{161}Tb]$TbCl_3$ product was assessed by radioTLC. Spotted Sorbtech (Norcross, GA) silica gel TLC plates with polyester backing (2.5 x 7.5 cm, 200 µm thickness) were developed with 0.1 M sodium citrate (pH = 5.5) and analyzed after drying on an Eckert & Ziegler radioTLC scanner.

To check for radionuclidic impurities in the final ^{161}Tb solution, an aliquot of approximately 1 µL was transferred to a 20 mL scintillation vial containing 10 mL of 0.1 M HCl solution. The resulting solution was analyzed using an HPGe detector.

2.8 Radiolabeling Assessments of the Final [^{161}Tb]$TbCl_3$ Product

2.8.1 DOTA Radiolabeling

The radiolabeling assessments were conducted via labeling reactions using a representative aliquot of the final [^{161}Tb]$TbCl_3$ solution and DOTA stock solutions of varying molar concentration in water ($3x10^{-6}$, $1x10^{-6}$, $5x10^{-7}$, $3x10^{-7}$, $1x10^{-7}$, and $5x10^{-8}$ M, along with 0 M as control). To microcentrifuge vials, 500 µL of the DOTA stock solutions were added,

followed by 20 µL of the diluted final ^{161}Tb solution (in 0.05 M HCl; 56 ± 4 µCi, 2.1 ± 0.1 MBq; n = 3). The reactions were heated for 60 min at 100 °C with mixing (900 rpm) on a pre-heated thermomixer. After cooling, the reactions were spotted on silica gel TLC plates that were then developed in 50:50 methanol: ammonium acetate (0.02 M, pH = 5.5) and measured on an Eckert & Ziegler radioTLC scanner.

2.8.2 DOTA-TATE Radiolabeling

Radiolabeling studies with the DOTA-TATE peptide were used to further assess the quality of the ^{161}Tb final product. To acid-washed plastic microcentrifuge tube, 86.6 µL of 0.2 M ammonium acetate (pH = 5.5) was added, followed by the addition of 28.4 µL of a DOTA-TATE stock solution (varying concentrations: 1.0, 0.10, 0.050, 0.038, and 0.025 mg/mL in water) and then 15 µL of [^{161}Tb]$TbCl_3$ in 0.05 M HCl (~43 µCi, ~1.6 MBq).

The reactions were heated for 45 min at 75 °C while mixing (900 rpm) on a preheated thermomixer. Subsequently, the radiolabeling yield was measured by HPLC, utilizing a BetaBasic™ C18 analytical column with a linear gradient of 15% to 40% acetonitrile in water (both with 0.1% trifluoroacetic acid) over 30 min and a flow rate of 1 mL/min. The [^{161}Tb]Tb-DOTA-TATE complex (retention time 15.2 min) was identified via co-injection with the non-radioactive Tb-DOTA-TATE reference standard (see below).

The Tb-DOTA-TATE standard was prepared by heating a solution consisting of 1 mL of DOTA-TATE in water (20 nmol), 0.53 mL of $TbCl_3$ in 0.05 M HCl (30 nmol), and 3.05 mL of 0.2 M ammonium acetate (pH = 5.5) at 75 °C for 45 min with mixing (900 rpm) on a pre-heated thermomixer. The HPLC retention time for the Tb-DOTA-TATE standard under the above-noted gradient conditions was 14.9 minutes, consistent with the tubing distance (and

thus volume) between the UV (first) and radiation (second) detectors. The Tb-DOTA-TATE standard was additionally characterized by HRMS. HRMS (m/z): calc. for $C_{65}H_{89}N_{14}O_{19}S_2Tb_1$, $[M + 2H]^{2+}$, 796.2556; found 796.2527 (see Supplementary Material Figure S1).

2.9 ICP-MS Analysis of the Final [^{161}Tb]$TbCl_3$ Product

Inductively Coupled Plasma Mass Spectrometry (ICP-MS) analyses were conducted using a PerkinElmer (Shelton, CT) NexION 300X ICP-MS with a Universal Cell operated in KED (Kinetic Energy Discrimination) mode, the acquisition method featuring two He flow groups: 2.5 mL He/min and 4.5 He/min. The instrument was calibrated with five linearity series prepared from commercial High Purity Standards (North Charleston, SC) single- and multi-element mixtures. All linearity standards and instrument blanks contained internal standards.

A 5 µL aliquot of each final ^{161}Tb product was transferred to an acid-washed 15 mL vial and stored for decay. The decayed sample was gravimetrically diluted with 0.45 M HNO_3. Serial dilutions were prepared as necessary to bring all analytes within the linear signal range of the ICP-MS. Internal standards Be, Sc, In, and Tl were added to all dilutions.

3. RESULTS AND DISCUSSION

3.1 Reactor Production of No-Carrier-Added ^{161}Tb

Direct production of ^{161}Tb via neutron irradiation is not practical given that ^{159}Tb is the only naturally abundant isotope of Tb and ^{160}Tb is long-lived (72 d half-life). In this work, an indirect method of producing ^{161}Tb was utilized, where neutron irradiation of ^{160}Gd (σ_{th} = 1.4 b) resulted in the production of the intermediate nuclide ^{161}Gd (3.66 min half-life),

which rapidly decays ^{161}Tb. Since the natural abundance of ^{160}Gd is only 22%, target preparation with enriched ^{160}Gd was used to minimize the co-production of radioactive impurities. Here, neutron irradiations of [^{160}Gd]Gd$(NO_3)_3$ targets (98.2% isotopic enrichment, Table 2) containing 1 mg of ^{160}Gd were conducted at MURR for 151 ± 3 h (n = 4) at a nominal thermal neutron flux of 1.76×10^{14} n·cm^{-2}·sec^{-1}, producing 19 ± 1 mCi (700 ± 40 MBq) of ^{161}Tb at the end of irradiation. [Place Table 2 near here]

Table 2: Target Material Isotopic Composition and Cross Sections for Gadolinium Isotopes Present.

Gd Isotope	152	154	155	156	157	158	160
Enrichment, %	<0.01	0.01	0.18	0.36	0.25	1.00	98.2 ± 0.1
Thermal Neutron Cross Section, Barns	735	85	60330	1.8	254000	2.2	1.4

The various Gd isotopes present in the target material (Table 2) resulted in the generation of both stable (^{155}Gd, ^{156}Gd, ^{157}Gd, ^{158}Gd) and radioactive (^{153}Gd, ^{159}Gd, ^{161}Gd) isotopes of gadolinium upon neutron irradiation. While the ^{159}Gd (and ^{153}Gd to a lesser extent) radioactive impurity provided a convenient radiotracer for Gd tracking throughout ^{161}Tb processing, the short-lived ^{161}Gd isotope was not observed due to its decay during the ~8-hour period between the end of irradiation and the start of processing. Other co-produced radioactive impurities also observed by HPGe spectroscopy (Table 3, Figure 2) were mainly due to the activation of elemental impurities present in the target material or from the decay of a co-produced radionuclidic impurity (i.e., ^{152}Eu resulting from the decay of ^{152m2}Eu). [Place Table 3 near here]

Table 3: Radionuclidic Impurities Observed in Irradiated Targets.

Radionuclidic Impurity	Radionuclidic Impurity Half-Life	Target Nuclear Reaction	Target Nuclide Natural Abundance, %	Target Nuclide Thermal Neutron Cross Section, Barns
^{24}Na	15.0 h	^{23}Na(n,γ)	100	0.53
^{141}Ce	32.5 d	^{140}Ce(n,γ)	88.5	0.51
^{153}Sm	46.3 h	^{152}Sm(n,γ)	26.7	206
^{152}Eu	13.5 y	^{151}Eu(n,γ)^{152m2}Eu→	47.8	9230
^{153}Gd	240 d	^{152}Gd(n,γ)	<0.01[a]	735
^{159}Gd	18.5 h	^{158}Gd(n,γ)	1.00[a]	2.2
^{160}Tb[b]	72.3 d	^{159}Tb(n,γ)	100	23.8
^{166}Ho	26.8 h	^{165}Ho(n,γ)	100	64.4
^{169}Yb	32.0 d	^{168}Yb(n,γ)	0.123	3033
^{175}Yb	4.19 d	^{174}Yb(n,γ)	32.0	63.2

Nuclear data was taken from Livechart - Table of Nuclides. [5]

[a] Abundance in isotopically enriched [^{160}Gd]Gd$(NO_3)_3$ target. [b] Resulting from activation of ^{159}Tb present in the [^{160}Gd]Gd$(NO_3)_3$ target (<2 ppm) and generated via decay of ^{159}Gd; observed in post-isolation ^{161}Tb samples after partial ^{161}Tb decay and/or measured with longer counting times.

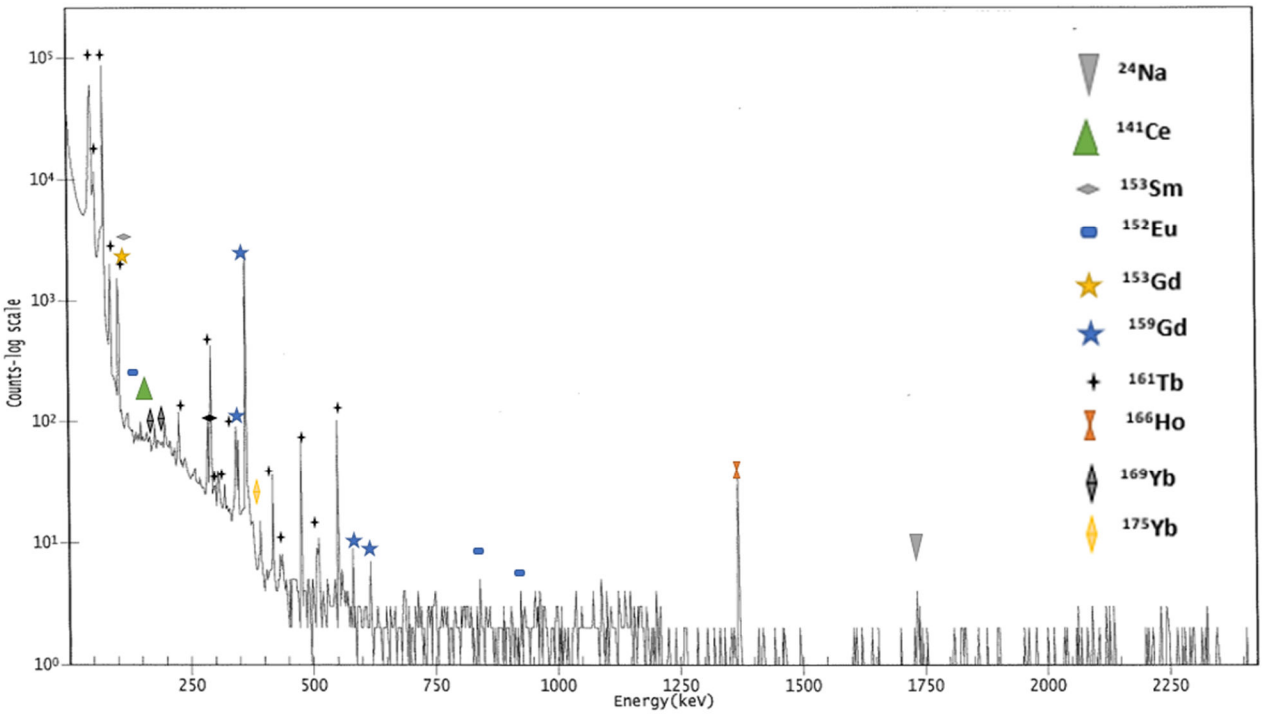

Figure 2: A typical gamma spectrum of irradiated target prior to ^{161}Tb isolation.

3.2 HPLC Isolation of ^{161}Tb

The cation-exchange HPLC column selected for the ^{161}Tb isolation process was comprised of a 10 µm polystyrene/divinylbenzene substrate agglomerated with cation-exchange latex. As noted earlier, the column separation is accomplished due to the propensity of positively charged ions to bind to the α-HIBA vs. the resin. The separation was highly sensitive to the pH of the α-HIBA mobile phase, and a pH of 3.3 was selected to isolate ^{161}Tb with a reasonable recovery while maintaining a practical elution time and volume. Higher pH values resulted in poorer separation between Tb and Gd due to reduced interaction with the cation-exchange resin, while lower pH values offered better resolution (and recovery, see below) but led to excessively long retention times as the lanthanides bound more strongly to the resin. Aliquots of irradiated targets dissolved in 0.1 M HCl (4.8 ±

0.6 mCi, 180 ± 20 MBq; n = 3, ~0.24 mg of ^{160}Gd mass) were loaded onto the HPLC column, and the ^{161}Tb peak was isolated from the Gd target material and radionuclidic impurities in 9-10 mL of 0.6 M α-HIBA using the live radiochromatogram (NaI(Tl) detector signal) to guide the collection (Figure 3). HPGe spectroscopy of collected fractions was used to identify the radionuclide(s) present in each peak. Due to the overlap between the peaks for Tb and the lighter lanthanides, the tail of the ^{161}Tb peak was not collected. While doing so resulted in high radionuclidic purity of the collected ^{161}Tb, it came at the cost of a lower recovery (59 ± 9%; 2.8 ± 0.6 mCi, 100 ± 20 MBq; n = 3). Additional modification of the HPLC collection method, such as by employing an optimized gradient, would likely increase the ^{161}Tb recovered from small quantity separations. However, even with such optimization, this method is only suitable for research-scale separations (i.e., low Gd masses) to yield ^{161}Tb activities in support of research and preclinical studies. Due to the low mass loading limitation of the HPLC isolation, it cannot be scaled to support production of clinically relevant ^{161}Tb quantities (i.e., processing of high Gd mass targets). Further method development would also be required to recover the expensive ^{160}Gd that is co-eluted in a large volume with various lighter lanthanides.

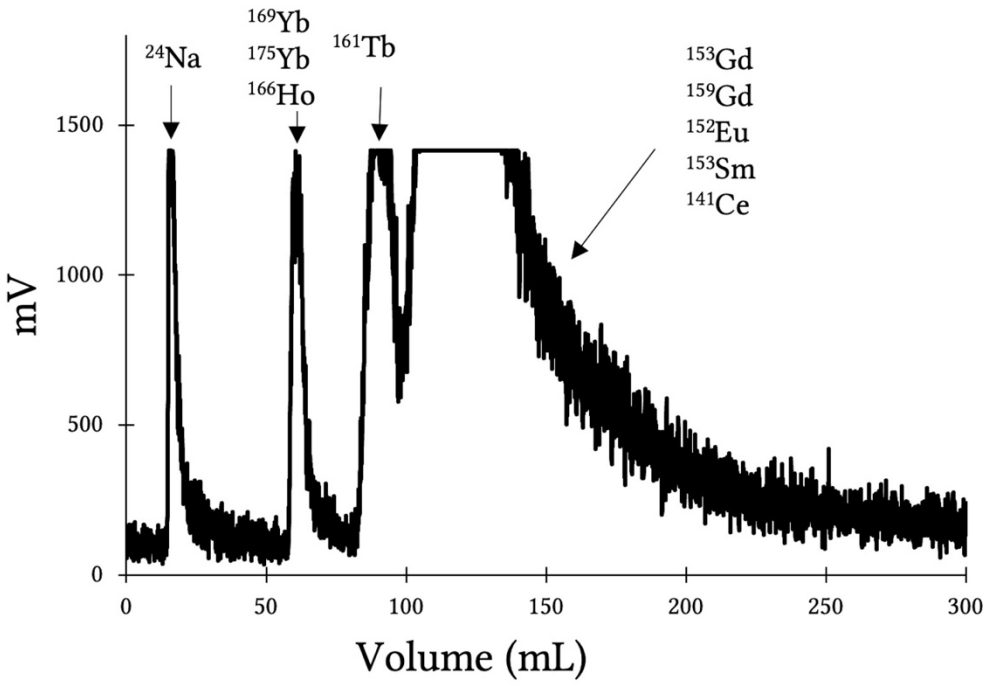

Figure 3: A typical radioHPLC chromatogram showing the NaI(Tl) detector signal used to guide isolation of ^{161}Tb from the Gd target material and radionuclidic impurities. Note: HPGe spectroscopy of collected fractions was used to determine the radionuclide(s) present in each peak.

3.3 Post-HPLC Processing and Final Formulation of ^{161}Tb

Following the cation-exchange HPLC separation, the isolated ^{161}Tb fraction was further purified using a packed LN resin column. The LN resin was selected for this step due to its stability in concentrated acids (up to 4 M HNO_3) and strong affinity for lanthanide ions, enabling efficient acid exchange from the α-HIBA eluant to HNO_3 without degradation of the resin or loss of binding capacity. The ^{161}Tb containing solution was loaded onto the packed LN column, which was then washed with water prior to eluting the ^{161}Tb in 3 M HNO_3 (Figure 4). The ^{161}Tb activity, recovered from the LN column in 1.00 mL of 3 M HNO_3, was 98 ± 1% of the loaded activity, equating to 2.7 ± 0.6 mCi (100 ± 20 MBq; n = 3) of isolated ^{161}Tb.

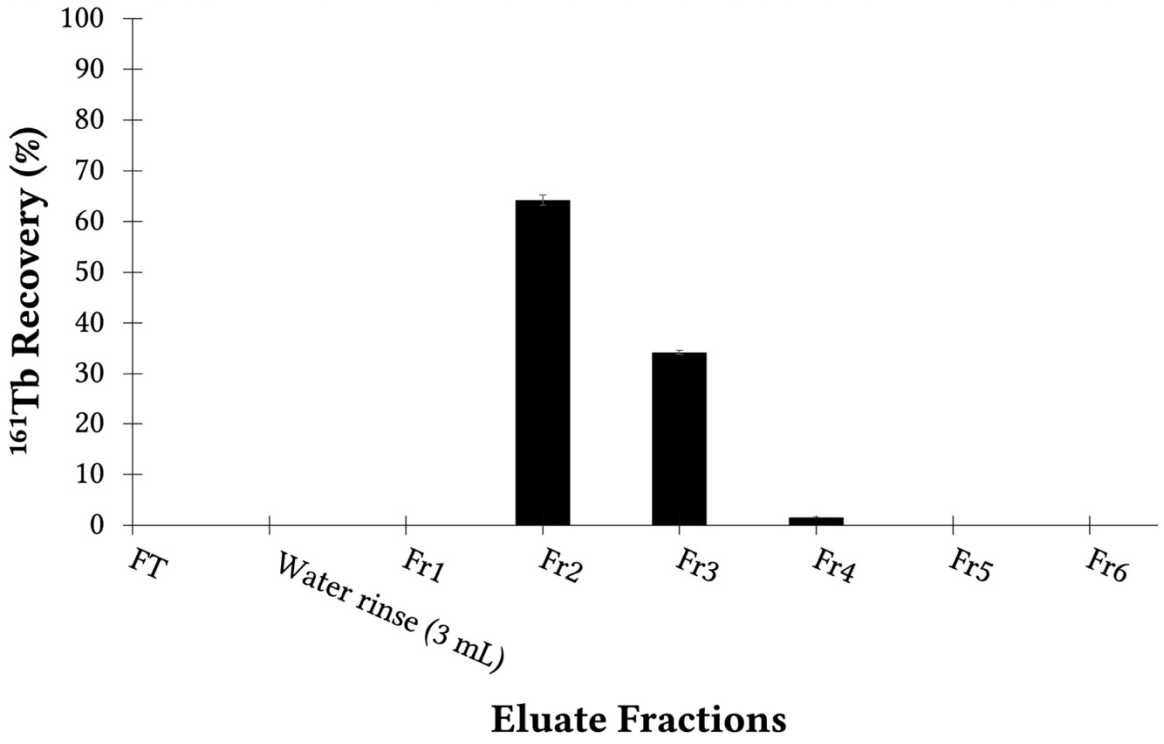

Figure 4: A typical elution profile of ^{161}Tb from the LN column (FT: flow through solution from column loading; Fr: fraction collected, 0.50 mL each).

The activity recovered from the LN column was then processed through a packed RE/PF resin-based column, to both remove organic contaminants and change the solvent from HNO_3 to HCl. Due to the high retention of trivalent lanthanide ions on RE resins, ^{161}Tb was retained on the RE resin in the 3 M HNO_3 loading step before being eluted in 0.05 M HCl from the PF resin, which trapped organic contaminants. No ^{161}Tb activity breakthrough was observed during loading, as shown in Figure 5, and the ^{161}Tb was eluted in this step with a 98.1 ± 0.1% recovery in 0.75-1.00 mL of 0.05 M HCl, equating to 2.6 ± 0.6 mCi (100 ± 20 MBq; n = 3).

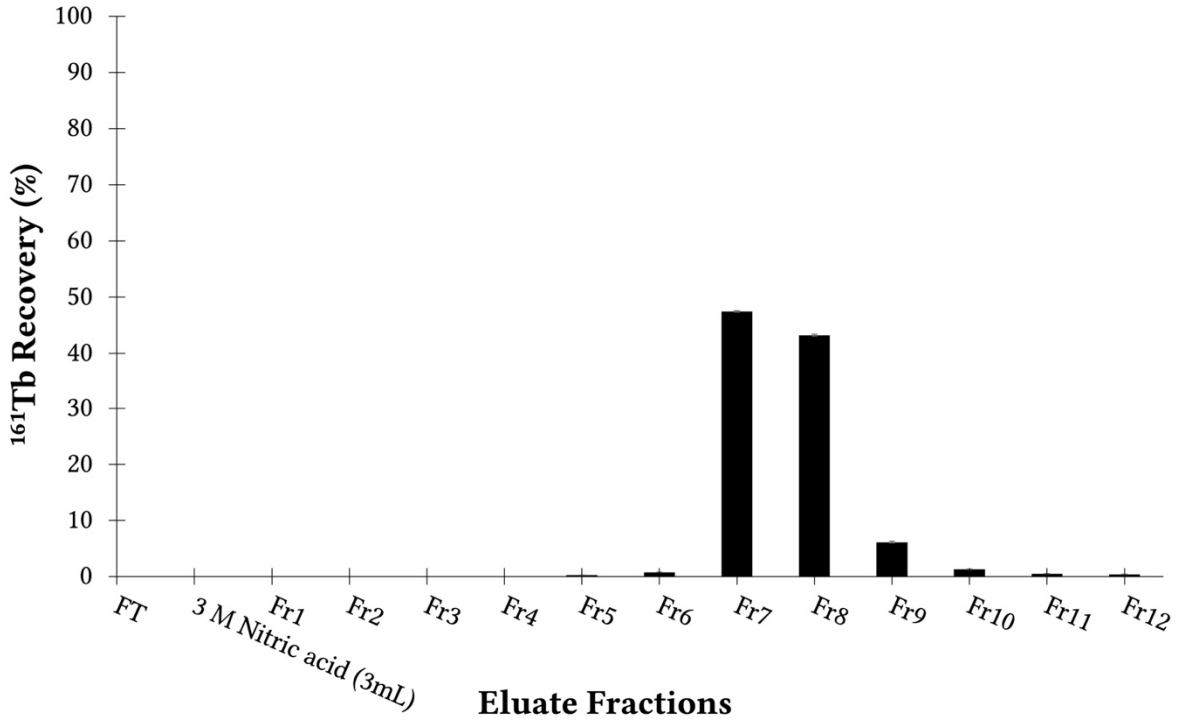

Figure 5: A typical elution profile of ^{161}Tb from the RE/PF column (FT: flow through solution from column loading; Fr: fraction collected, 0.25 mL each).

To drive off residual HNO_3 and concentrate the recovered ^{161}Tb, the final step involved repeated solvent evaporation and reconstitution of the ^{161}Tb, using a silanized vial to avoid activity loss. This resulted in a final formulation of ^{161}Tb in 150 µL of 0.05 M HCl (55 ± 7% overall recovery, pH = 1.3) for product quality assessments, including radiolabeling studies.

The moderate overall recovery of 55 ± 7% achieved with this method, which resulted from the modest recovery of the HPLC step, was lower than other ^{161}Tb purification methods reported in the literature. For example, Gracheva et al. achieved 80-90% recovery using a two-column purification method combining Sykam and LN3 resin columns.[18] Holiski et al. demonstrated successful ^{161}Tb separation from large-scale targets (>200 mg) using a comprehensive scheme combining cation exchange (AG 50W-X8) and extraction

chromatography (bDGA and LN) resins, achieving >89% recovery.[20] Brezovcsik et al. reported 85 ± 2% and 93 ± 2% recoveries using analytical and semi-preparative columns, respectively, both employing AG50W-X8 cation exchange resin.[14]

Notwithstanding the moderate recovery, this HPLC-based approach reproducibly yielded ^{161}Tb in an amount and formulation suitable for research and preclinical studies. Further, the total processing time from irradiated target dissolution to final formulated product was only ~5 h, with the HPLC isolation requiring ~2 h, the post-HPLC column purification steps taking ~2 h, and the final formulation needing ~1 h. This processing time was very practical given the ^{161}Tb half-life of 6.95-day.

3.4 Radiochemical and Radionuclidic Purity Assessments

Radiochemical purity was assessed by radioTLC analysis of silica gel TLC plates spotted with the final ^{161}Tb solution and developed in 0.1 M sodium citrate. The citrate complex formed with $^{161}Tb^{3+}$ results in an R_f value of 0.6, whereas colloidal ^{161}Tb remains at the origin (R_f of 0). High radiochemical purity (>99%, n = 3) was observed for the final ^{161}Tb product (see Supplementary Material Figure S2).

HPGe spectroscopy was utilized for radionuclidic purity assessment of the final ^{161}Tb solution. The signals from the numerous radionuclide impurities observed in the dissolved irradiated target (Figure 2), most notably that of ^{159}Gd at 363 keV, were absent on the gamma spectrum of the final ^{161}Tb solution (Figure 6), confirming the high radionuclidic purity achieved by the isolation process. As expected, the co-produced ^{160}Tb isotope resulting from activation of ^{159}Tb (Table 3) both present in the [^{160}Gd]Gd(NO_3)$_3$ target (<2 ppm, see

Supplementary Material Table S1) and generated via decay of ^{159}Gd, could be observed after partial ^{161}Tb decay and/or in measurements with longer counting times.

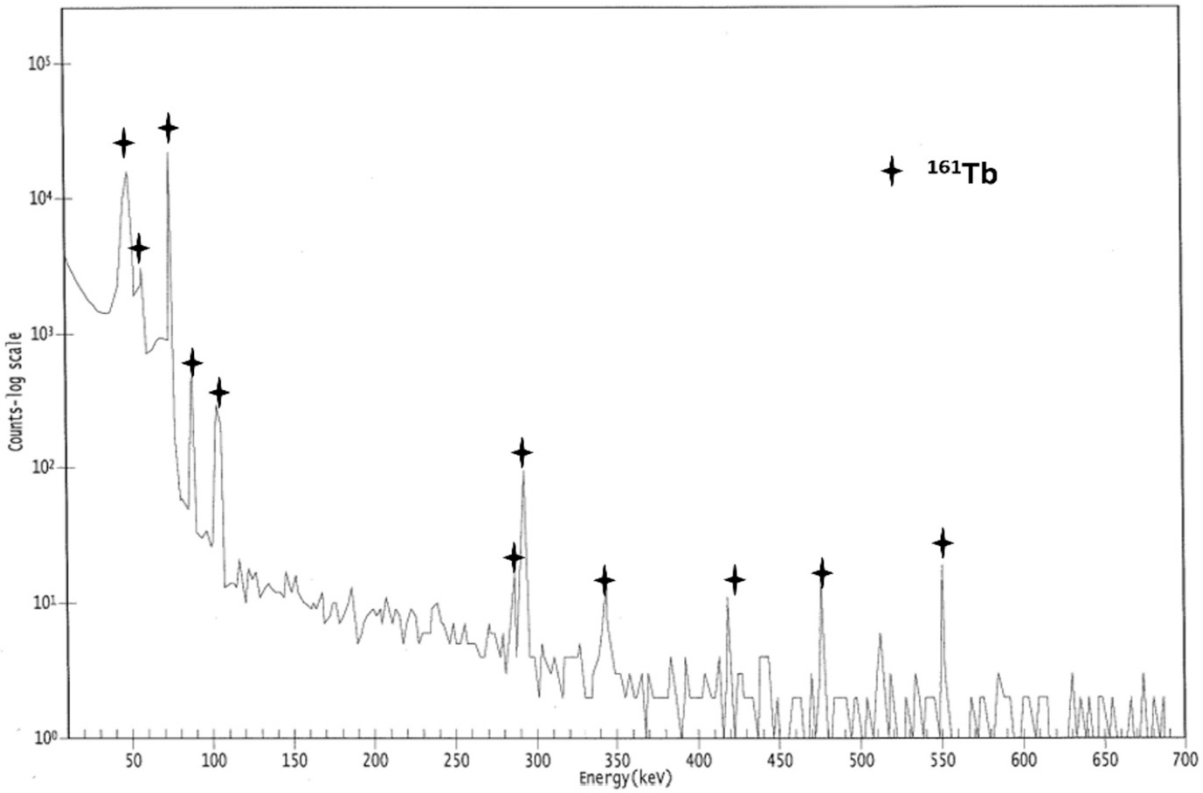

Figure 6: A typical gamma spectrum of final ^{161}Tb product solution. Measurement conditions: 600-sec acquisition time at 13 h post end of irradiation of sample located 3 cm from detector.

3.5 Radiolabeling Assessments

The suitability of the final ^{161}Tb solution for radiolabeling studies was evaluated via reactions with the "gold standard" DOTA chelator. The radiolabeling yields resulting from reacting ^{161}Tb with varying DOTA concentrations were measured by radioTLC analysis using spotted silica gel plates developed in a 50:50 methanol: ammonium acetate (0.02 M, pH 5.5) solution. The R_f value of the radiolabeled [^{161}Tb]Tb-DOTA complex was 0.5-0.6, while the R_f value of unlabeled ^{161}Tb was 0. The maximum apparent molar activity (AMA) of labeling

obtained for the [^{161}Tb]Tb-DOTA complex was 202-336 μCi/nmol (7.5-12.4 MBq/nmol; n = 3, Figure 7).

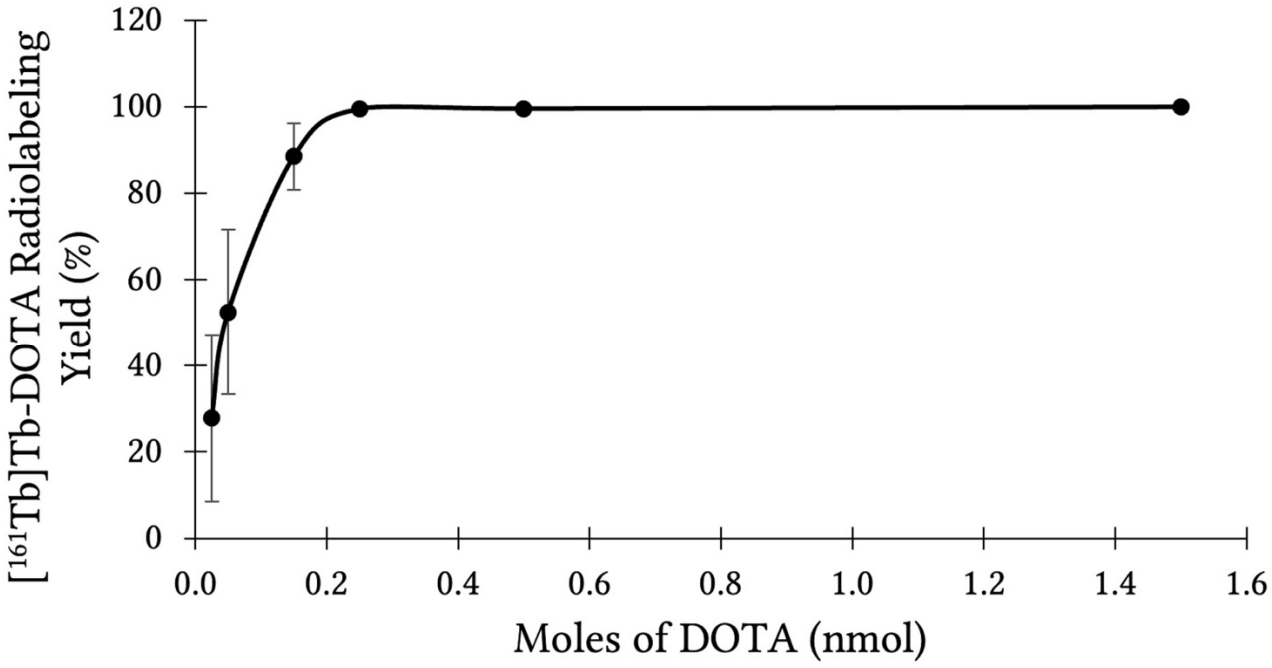

Figure 7: Effect of varying moles of DOTA on radiolabeling yield with ^{161}Tb (56 ± 4 μCi, 2.1 ± 0.1 MBq; n = 3).

Additional quality assessments of the ^{161}Tb final product were performed via DOTA-TATE radiolabeling studies. The use of the DOTA-TATE peptide has been well-established in the literature for evaluating the radiolabeling efficiency of various radiometals, including ^{90}Y and ^{177}Lu. Furthermore, clinical studies have demonstrated the successful application of DOTA-TATE in nuclear medicine via its radiometalated complexes, such as the FDA approved radiopharmaceuticals NETSPOT™ (^{68}Ga) and LUTATHERA® (^{177}Lu). Here, HPLC analyses were used to measure the ^{161}Tb radiolabeling yields. The [^{161}Tb]Tb-DOTA-TATE complex was identified by its co-elution with the characterized non-radioactive Tb-DOTA-TATE standard (Figure 8). The maximum AMA of ^{161}Tb labeling was determined to be 80-100

μCi/nmol (3.0-3.7 MBq/nmol) for reactions conducted at an activity concentration of 2.7-3.3 μCi/μL (0.10-0.12 MBq/μL). Comparatively higher results have been reported in the literature for similar peptides, such as the 1400 μCi/nmol (50 MBq/nmol) AMA obtained for ^{161}Tb radiolabeling of DOTA-TOC; however, this was achieved with a significantly higher activity concentration of 14 μCi/μL (0.5 MBq/μL).[18] The lower AMA of labeling here is likely due to both the lower ^{161}Tb reaction activity concentration as well as metal impurities in the final product (see section 3.6 below).

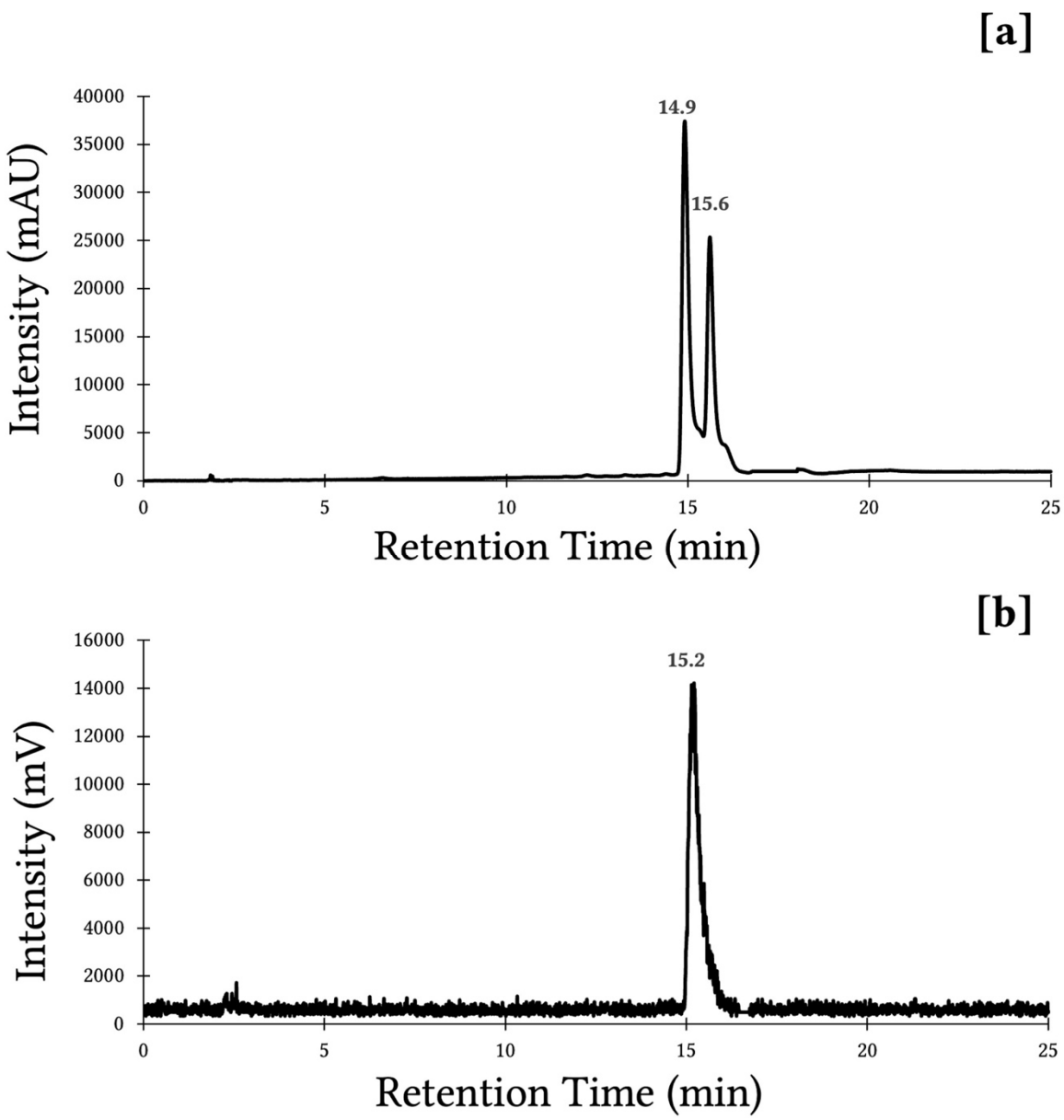

Figure 8: Typical HPLC chromatograms from co-injection of the non-radioactive Tb-DOTA-TATE standard with the [^{161}Tb]Tb-DOTA-TATE radiocomplex. Panel [a] shows the Tb-DOTA-TATE standard at 14.9 min and the unlabeled DOTA-TATE peptide at 15.6 min (UV, 280 nm). Panel [b] shows the [^{161}Tb]Tb-DOTA-TATE complex at 15.2 min (RAD).

3.6 ICP-MS Analysis of the Final ^{161}Tb Product

Samples of the final ^{161}Tb solutions were stored for decay prior to determining their isotopic and elemental compositions by ICP-MS analysis. The results presented in Table 4 show that the only lanthanide isotopes measured with concentrations above the limit of detection (LOD) were ^{159}Tb and ^{161}Dy, consistent with the successful removal of other lanthanides during ^{161}Tb isolation. The presence of ^{161}Dy was from the decay of ^{161}Tb, while the presence of ^{159}Tb was attributed to the ^{nat}Tb (monoisotopic as ^{159}Tb) impurity in the Gd target material (see Supplementary Material Table S1) as well as from decay of the co-produced ^{159}Gd radionuclide. Measurable concentrations were observed for several transition metals that can compete with ^{161}Tb during the DOTA radiolabeling process (Table 5). The transition metal impurities observed in our study were consistent with those reported for final ^{161}Tb products in the literature, likely introduced during the purification process or from external environmental contamination.[5,18] The presence of lanthanide and transition metals lowers the maximum AMA of radiolabeling, particularly when using DOTA/DOTA-TATE, by competing with the radiometal for chelator binding. Future optimization studies should focus on incorporating an additional step, such as the use of a diglycolamide (DGA) resin, to reduce transition metal impurities in the final solution and potentially increase the achievable AMA. [Place Tables 4 and 5 near here]

Table 4: A Typical ICP-MS Analysis of Lanthanides Present in the Decayed Final ^{161}Tb Product.

Element*	La	Ce	Pr	Nd	Sm	Eu	^{nat}Gd	^{160}Gd
Measured, ppb	<LOD	<LOD	<LOD	<LOD	<LOD	<LOD	<LOD	<LOD
LOD, ppb	0.38	0.49	0.18	0.46	1.5	0.14	0.61	0.19

Element*	^{159}Tb	^{161}Dy	^{nat}Dy	Ho	Er	Tm	Yb	Lu
Measured, ppb	1.3	25.8	<LOD	<LOD	<LOD	<LOD	<LOD	<LOD
LOD, ppb	0.095	0.099	0.90	0.075	0.32	0.11	1.2	0.35

LOD = limit of detection; *Pm has no stable isotope.

Table 5: A Typical ICP-MS Analysis of First-Row Transition Metals Present in the Decayed Final ^{161}Tb Product.

Element	Ca	Ti	V	Cr	Mn	Fe	Co	Ni	Cu	Zn
Measured, ppb	<LOD	43	<LOD	30	6.5	1190	1.1	329	10.1	160
LOD, ppb	3500	29	2.5	13	6.3	120	0.83	7.8	1.6	9.9

LOD = limit of detection.

Conclusions

Separating adjacent lanthanides, such as ^{161}Tb produced from neutron irradiation of ^{160}Gd, is challenging due to their similar physical and chemical properties. The separation method presented herein involved an initial ^{161}Tb isolation step using cation-exchange HPLC, in which pH control was key, followed by an acid-exchange step via an LN resin-based column prior to organic contaminant removal with a RE/PF resin-based column. The high radiochemical and radionuclidic purities of the resulting ^{161}Tb solution in 0.05 M HCl, along with its successful use in radiolabeling the DOTA chelator and the DOTA-TATE peptide, demonstrated that the overall process was effective in producing quality ^{161}Tb. While this processing method was successfully applied at research scale quantities of ^{161}Tb, the low

mass tolerance of the HPLC isolation step precludes application of this method to clinically relevant production scales.

Acknowledgments

This material is based upon work supported by the U.S. Department of Energy, Office of Science, Office of Isotope R&D and Production program under Award Number DE-SC0022235. Additional support was provided by the University of Missouri-Columbia (MU Research Reactor and Department of Chemistry). We acknowledge the National Science Foundation for the award BCS-0922374 to the University of Missouri, which funded the ICP-MS equipment used in this research.

Disclaimer

References

(1) *FDA Letter of Approval for NETSPOT™*. https://www.accessdata.fda.gov/drugsatfda_docs/appletter/2016/208547Orig1s000ltr.pdf (accessed 2024-08-20).

(2) *FDA Letter of Approval for LUTATHERA®*. https://www.accessdata.fda.gov/drugsatfda_docs/appletter/2018/208700Orig1s000ltr.pdf (accessed 2024-08-20).

(3) Hofling, A. A.; Fotenos, A. F.; Niu, G.; Fallah, J.; Agrawal, S.; Wang, S.-J.; Marzella, L. Prostate Cancer Theranostics: Concurrent Approvals by the Food and Drug Administration of the First Diagnostic Imaging Drug Indicated to Select Patients for a Paired Radioligand Therapeutic Drug. *J. Nucl. Med.* **2022**, *63*(11):1642–1643. https://doi.org/10.2967/jnumed.122.264299.

(4) Langbein, T.; Weber, W. A.; Eiber, M. Future of Theranostics: An Outlook on Precision Oncology in Nuclear Medicine. *J Nucl Med* **2019**, *60* (Supplement 2), 13S-19S. https://doi.org/10.2967/jnumed.118.220566.

(5) Lehenberger, S.; Barkhausen, C.; Cohrs, S.; Fischer, E.; Grünberg, J.; Hohn, A.; Köster, U.; Schibli, R.; Türler, A.; Zhernosekov, K. The Low-Energy β^- and Electron Emitter ^{161}Tb as an Alternative to ^{177}Lu for Targeted Radionuclide Therapy. *Nucl. Med. Biol.* **2011**, *38* (6), 917–924. https://doi.org/10.1016/j.nucmedbio.2011.02.007.

(6) *Livechart - Table of Nuclides - Nuclear structure and decay data*. https://www-nds.iaea.org/relnsd/vcharthtml/VChartHTML.html (accessed 2024-08-20).

(7) Müller, C.; Fischer, E.; Behe, M.; Köster, U.; Dorrer, H.; Reber, J.; Haller, S.; Cohrs, S.; Blanc, A.; Grünberg, J.; Bunka, M.; Zhernosekov, K.; van der Meulen, N.; Johnston, K.; Türler, A.; Schibli, R. Future Prospects for SPECT Imaging Using the Radiolanthanide Terbium-155 – Production and Preclinical Evaluation in Tumor-Bearing Mice. *Nucl. Med. Biol.* **2014**, *41*, e58–e65. https://doi.org/10.1016/j.nucmedbio.2013.11.002.

(8) Müller, C.; Umbricht, C. A.; Gracheva, N.; Tschan, V. J.; Pellegrini, G.; Bernhardt, P.; Zeevaart, J. R.; Köster, U.; Schibli, R.; van der Meulen, N. P. Terbium-161 for PSMA-Targeted Radionuclide Therapy of Prostate Cancer. *Eur. J. Nucl. Med. Mol. Imaging* **2019**, *46* (9), 1919–1930. https://doi.org/10.1007/s00259-019-04345-0.

(9) Müller, C.; Reber, J.; Haller, S.; Dorrer, H.; Bernhardt, P.; Zhernosekov, K.; Türler, A.; Schibli, R. Direct *In Vitro* and *In Vivo* Comparison of ^{161}Tb and ^{177}Lu Using a Tumour-Targeting Folate Conjugate. *Eur. J. Nucl. Med. Mol. Imaging.* **2014**, *41* (3), 476–485. https://doi.org/10.1007/s00259-013-2563-z.

(10) Baum, R. P.; Singh, A.; Kulkarni, H. R.; Bernhardt, P.; Rydén, T.; Schuchardt, C.; Gracheva, N.; Grundler, P. V.; Köster, U.; Müller, D.; Pröhl, M.; Zeevaart, J. R.; Schibli, R.; van der Meulen, N. P.; Müller, C. First-in-Humans Application of ^{161}Tb: A Feasibility Study Using ^{161}Tb-DOTATOC. *J. Nucl. Med.* **2021**, *62* (10), 1391–1397. https://doi.org/10.2967/jnumed.120.258376.

(11) Schaefer-Schuler, A.; Burgard, C.; Blickle, A.; Maus, S.; Petrescu, C.; Petto, S.; Bartholomä, M.; Stemler, T.; Ezziddin, S.; Rosar, F. [^{161}Tb]Tb-PSMA-617 Radioligand Therapy in Patients with mCRPC: Preliminary Dosimetry Results and Intra-Individual Head-to-Head Comparison to [^{177}Lu]Lu-PSMA-617. *Theranostics* **2024**, *14* (5), 1829–1840. https://doi.org/10.7150/thno.92273.

(12) Van de Voorde, M.; Van Hecke, K.; Cardinaels, T.; Binnemans, K. Radiochemical Processing of Nuclear-Reactor-Produced Radiolanthanides for Medical Applications. *Coord. Chem. Rev.* **2019**, *382*, 103–125. https://doi.org/10.1016/j.ccr.2018.11.007.

(13) Knapp, F. F.; Dash, A. Reactor-Produced Therapeutic Radionuclides. In *Radiopharmaceuticals for Therapy*; Springer India: New Delhi, 2016; pp 71–113. https://doi.org/10.1007/978-81-322-2607-9.

(14) Brezovcsik, K.; Kovács, Z.; Szelecsényi, F. Separation of Radioactive Terbium from Massive Gd Targets for Medical Use. *J. Radioanal. Nucl. Chem.* **2018**, *316* (2), 775–780. https://doi.org/10.1007/s10967-018-5718-3.

(15) Cieszykowska, I.; Żółtowska, M.; Mielcarski, M. Separation of Ytterbium from ^{177}Lu/Yb Mixture by Electrolytic Reduction and Amalgamation. *SOP Trans. Appl. Chem.* **2014**, *1* (2), 6–13. https://doi.org/10.15764/stac.2014.02002.

(16) Van So, L.; Morcos, N.; Zaw, M.; Pellegrini, P.; Greguric, I. Alternative Chromatographic Processes for No-Carrier Added ^{177}Lu Radioisotope Separation: Part I. Multi-Column Chromatographic Process for Clinically Applicable. *J. Radioanal. Nucl. Chem.* **2008**, *277* (3), 663–673. https://doi.org/10.1007/s10967-007-7129-8.

(17) Lebedev, N. A.; Novgorodov, A. F.; Misiak, R.; Brockmann, J.; Rösch, F. Radiochemical Separation of No-Carrier-Added ^{177}Lu as Produced via the ^{176}Yb(n,γ)^{177}Yb→^{177}Lu Process. *Appl. Radiat. Isot.* **2000**, *53* (3). 421-425. https://doi.org/10.1016/s0969-8043(99)00284-5.

(18) Gracheva, N.; Müller, C.; Talip, Z.; Heinitz, S.; Köster, U.; Zeevaart, J. R.; Vögele, A.; Schibli, R.; Van Der Meulen, N. P. Production and Characterization of No-Carrier-Added ^{161}Tb as an Alternative to the Clinically Applied ^{177}Lu for Radionuclide Therapy. *EJNMMI Radiopharm. Chem.* **2019**, 4–12. https://doi.org/10.1186/S41181-019-0063-6.

(19) Pourjavid, M. R.; Norouzi, P.; Rashedi, H.; Ganjali, M. R. Separation and Direct Detection of Heavy Lanthanides Using New Ion-Exchange Chromatography: Fast Fourier Transform

Continuous Cyclic Voltammetry System. *J. Appl. Electrochem.* **2010**, *40* (9), 1593–1603. https://doi.org/10.1007/s10800-010-0144-4.

(20) Holiski, C. K.; Bender, A. A.; Monte, P. F.; Hennkens, H. M.; Embree, M. F.; Wang, M.-J. (vince); Sjoden, G. E.; Mastren, T. The Production and Separation of ^{161}Tb with High Specific Activity at the University of Utah. Appl. Radiat. Isot. 2024, 214 (111530), 111530. https://doi.org/10.1016/j.apradiso.2024.111530.

Title: Production and Purification of Research Scale ^{161}Tb Using Cation-Exchange Semi-Preparative HPLC for Radiopharmaceutical Applications

Short title: Purification of Reactor-Produced ^{161}Tb via Cation-Exchange HPLC

Patrick Bokolo[1], Madhushan Serasinghe[1], Marina Kuchuk[2], Jim Guthrie[2], Mary Embree[2], Stacy Wilder[2], Dmitri G. Medvedev[3], Cathy S. Cutler[3], D. Scott Wilbur[4], Yawen Li[4], Carolyn J. Anderson[1,5,6,7], Silvia S. Jurisson[1], Heather M. Hennkens[1,2*]

1. Department of Chemistry, University of Missouri, Columbia, 65211, MO, USA
2. Research Reactor Center (MURR), University of Missouri, Columbia, 65211, MO, USA
3. Isotope Research and Production Department, Brookhaven National Laboratory, Upton, 11973, NY, USA
4. Department of Radiation Oncology, University of Washington, Seattle, 98195, WA, USA
5. Department of Radiology, University of Missouri, Columbia, 65211, MO, USA
6. Molecular Imaging and Theranostics Center, University of Missouri, Columbia, 65211, MO, USA
7. Ellis Fischel Cancer Center, University of Missouri, Columbia, 65211, MO, USA

* Author to whom correspondence should be addressed.
E-Mail: HennkensH@missouri.edu; Address: Department of Chemistry, University of Missouri, 601 South College Avenue, Columbia, MO, 65211, United States

Table S1: Chemical impurities of [^{160}Gd]Gd_2O_3 target material as reported from Trace Sciences International.

Element	K	Na	Ca	Mg	Fe	Al	Si	Cr	Ni	Cu	Tb	Dy	Er
ppm	<50	<20	<50	<3	>50	<3	<50	<5	<1	<1	<2	<1	<1

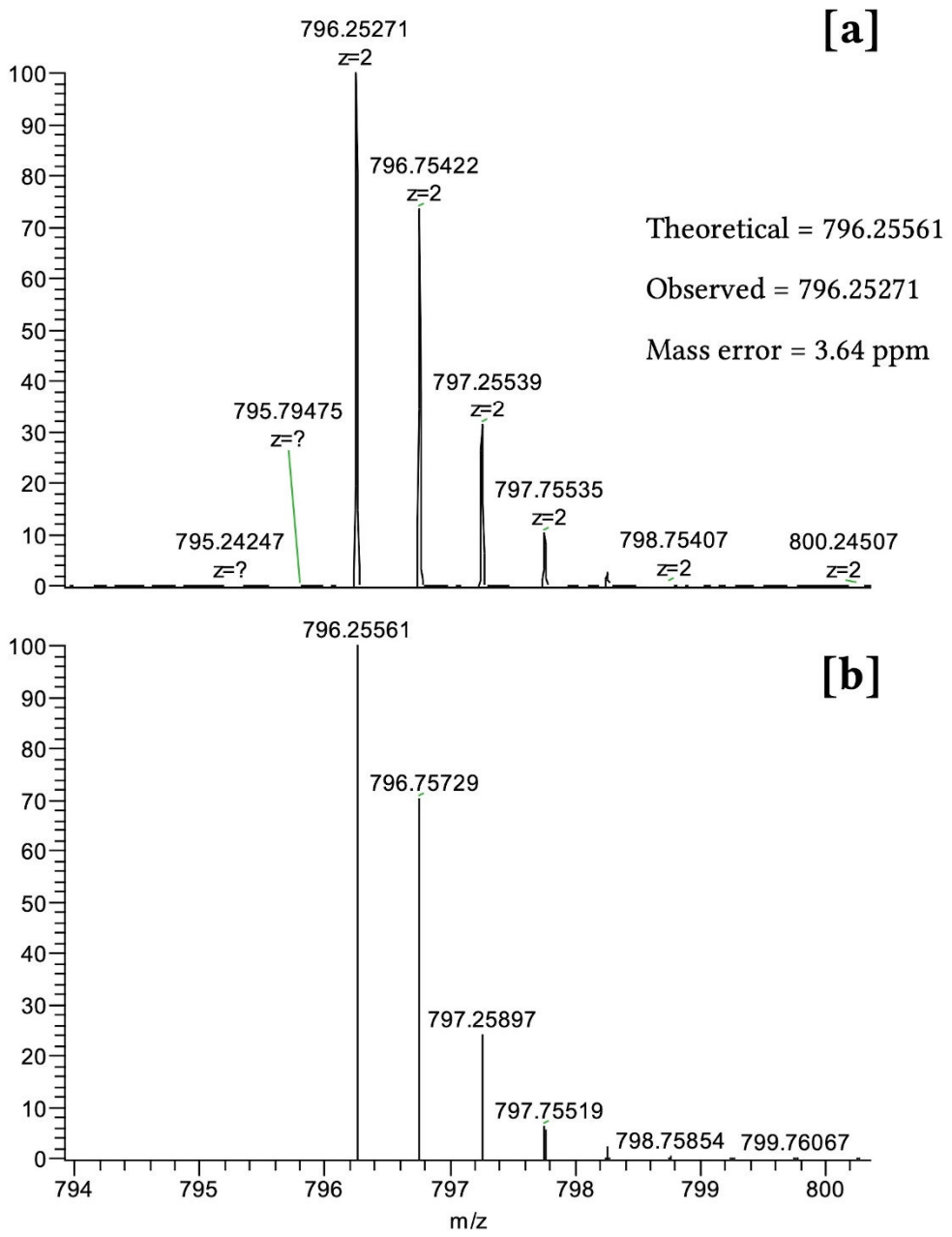

Figure S1: HRMS analysis of the non-radioactive Tb-DOTA-TATE standard. Panel [a] shows the observed *m/z*. Panel [b] shows the theoretical *m/z* for $C_{65}H_{89}N_{14}O_{19}S_2Tb_1$, $[M+2H]^{2+}$.

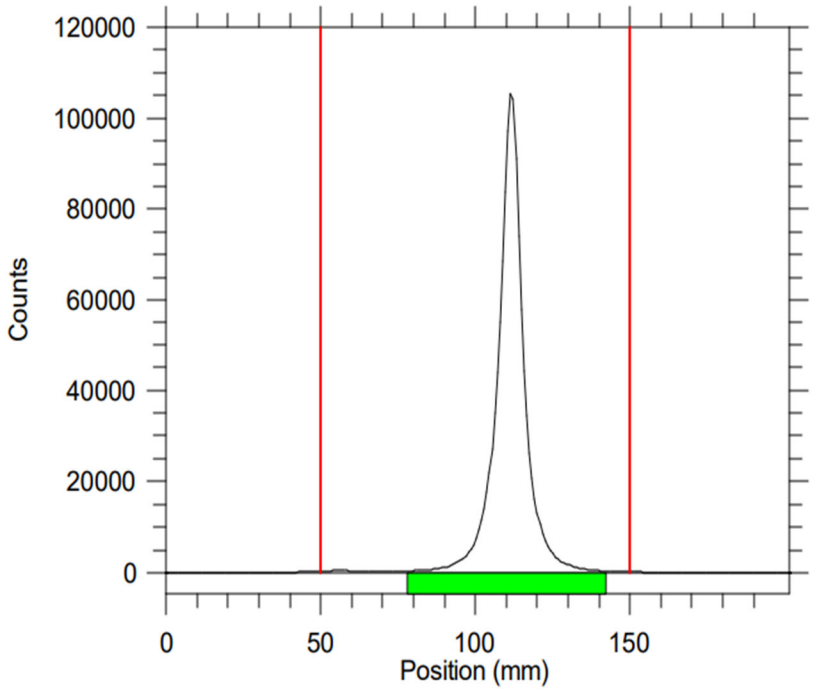

Figure S2: A typical radioTLC of final ^{161}Tb product for radiochemical purity determination.

Silanization Procedure

The silanization of glass vials involved immersing the vials in a 2% v/v solution of dimethyldichlorosilane in chloroform for 10 min. Following air-drying of the treated glass vials, they were heated in an oven for 2 h at 70-75 °C. The glass vials were then rinsed with 18 MΩ water, dried in air, and stored at room temperature.